

## Fabrication of Structured Porous Film by Electrophoresis

Zhong-Ze Gu,<sup>†</sup> Sinya Hayami,<sup>†</sup> Syoichi Kubo,<sup>‡</sup>  
Qing-Bo Meng,<sup>†</sup> Yasuaki Einaga,<sup>‡</sup> Donald A. Tryk,<sup>‡</sup>  
Akira Fujishima,<sup>‡</sup> and Osamu Sato<sup>†,\*</sup>

Kanagawa Academy of Science and Technology  
KSP Building East 412, 3-2-1 Sakado  
Takatsu-ku, Kawasaki-shi, Kanagawa 213-0012, Japan  
Department of Applied Chemistry  
School of Engineering, The University of Tokyo  
7-3-1 Hongo, Bunkyo-ku, Tokyo 113-8565, Japan

Films with three-dimensionally ordered macroporous structures have recently been studied extensively because of their wide applications in separations, catalysis, optical information processing, and microwave shielding.<sup>1–4</sup> A number of methods have been developed for the fabrication process, among which the template replication of opal films provides a simple, efficient path. The sol–gel method was the first to be used to replicate opal templates and has become one of the most popular methods currently used for fabricating porous materials.<sup>4–6</sup> Other methods, including CVD,<sup>7</sup> electrochemical deposition,<sup>8,9</sup> and hydrodynamic infiltration of nanoparticles,<sup>10</sup> have also been developed for the purpose of fabricating high-quality porous films with materials that cannot be prepared by the sol–gel method. An additional, recently developed technique involves the co-sedimentation of micrometer-scale template particles and nanoparticles.<sup>11,12</sup> However, the challenge remains to produce porous materials with long-range order and large single domains, which are essential for many of the possible applications. The key point is how to completely infiltrate an opal template with a low-shrinkage material without destroying the ordering of the opal. In this paper, we demonstrate that electrophoresis, which was used as a method to pack colloidal particles closely on substrate,<sup>13,14</sup> is a promising new technique for the preparation of high-quality inverse opals. In this technique, an electric field is used to fill the voids of the opal template with nanoparticles, for example, silica or titania, to form the inverse opal. This approach has several advantages. First, the nanoparticles themselves, because they are already fully dense, do not contribute to shrinkage. During the electrophoresis, they fill the voids of the opal freely and completely under the influence of the external field. Such field-induced filling packs the nanoparticles into the voids very tightly, which further decreases the shrinkage originating from the rearrangement of the nanoparticles during calcination. Second, the field-induced filling of nanoparticles is

quite fast. Only a few minutes are needed to fill an opal with a thickness of 10  $\mu\text{m}$ , which is much less than that for previously reported filling methods. Third, because there is no crystal growth involved, there is no need for nucleation, and therefore the filling can proceed uniformly. As a result, high-quality inverse opals with flat surfaces and large domains can be prepared. The area of a single crack-free domain of an inverse opal prepared in this way can exceed 10 000  $\mu\text{m}^2$ . A fourth advantage can be expected to be that the electrophoresis technique should be suitable for all materials that can be prepared in nanoparticle form, regardless of conductivity.

The electrophoresis was carried out in a two-electrode electrolytic cell. An ITO glass sheet covered with an opal template was used as the working electrode, and a platinum plate was used as the counter electrode. The opal films on the ITO glass were prepared by vertical deposition (i.e., dip-coating).<sup>15</sup> Monodisperse polystyrene spheres (Duke Scientific, U.S.A., and Polysciences Inc., U.S.A.) with diameters  $D$  between 200 and 800 nm were used. The two electrodes were placed parallel to each other to obtain a uniform electric field. The distance between the electrodes was 2 cm. The electrophoresis was performed at constant voltages of 10–20 V. Voltage in this range produced the highest quality inverse opals. Higher voltages can induce water electrolysis and, as a result, destroy the opal film. Conversely, lower voltages did not provide sufficient force to completely fill the pores. For the electrophoresis,  $\sim 10\%$  aqueous suspensions of silica (6 nm) and titania (15 nm) (Catalysts & Chemicals Ind. Co., Japan) were used. In opals, three types of voids exist; the smallest has a diameter of  $0.15D$ . For example, for an opal composed of 200-nm spheres, nanoparticles smaller than 30 nm can freely penetrate the voids and fill them. Because even low concentrations of ions in solution can facilitate water electrolysis at relatively low voltages, the nanoparticle suspensions were deionized before use.  $\zeta$ -Potential measurements showed that the surface charges of the silica and titania nanoparticles are negative. Thus, positive voltages were applied to the ITO electrode to infiltrate the opal template and fill it. Typically, 8 min of electrophoresis was performed for a template with a thickness of 10  $\mu\text{m}$ . After electrophoresis, the samples were dried in air. Finally, calcination at 450  $^\circ\text{C}$  in air was used to both remove the polystyrene spheres and sinter the oxide nanoparticles.

Figure 1 shows an SEM image of an inverse opal replicated using silica nanoparticles. A flat surface with a regular hexagonal structure was observed over a large area, indicating that the opal template was well replicated. The hexagonal ordering can be assigned to the (111) plane of the CCP structure.<sup>2,4,15</sup> The center-to-center distances between neighboring air spheres were found to be 256, 419, 531, and 621 nm for templates with sphere sizes of 263, 426, 542, and 640 nm. The average shrinkage was thus about 3%. This value is much smaller than those typical for the sol–gel method, for which the shrinkage is usually 20–30%.<sup>8</sup> Because the nanoparticles pack tightly under the influence of the electric field, the shrinkage here is also smaller than that for samples prepared by other nanoparticle-infiltration methods, for example,  $\sim 5\%$  for co-sedimentation.<sup>5,6</sup> No pinholes were observed in the silica network, indicating that the filling by the silica nanoparticles was complete. It is important to note here that the average distance between cracks, which is one of the most important quality indices for inverse opals, was  $\sim 30 \mu\text{m}$ . This value is even better than the opal template itself, which is vulnerable to cracking under vacuum. Single domains without cracks can be found with areas exceeding 10 000  $\mu\text{m}^2$ .

From a high magnification SEM image (Figure 1a, inset), the second layer, which can be viewed clearly through the top layer

(15) Jiang, P.; Bertone, J. F.; Hwang, K. S.; Colvin, V. L. *Chem. Matter.* **1999**, *11*, 2132–2140.

<sup>†</sup> Kanagawa Academy of Science and Technology.

<sup>‡</sup> The University of Tokyo.

(1) Yablonovitch, E. *Phys. Rev. Lett.* **1987**, *58*, 2059–2062.

(2) Xia, Y.; Gates, B.; Yin, Y.; Lu, Y. *Adv. Mater.* **2000**, *12*, 693–713.

(3) Soukoulis, C. M. *Photonic Band Gap Materials*; Kluwer Academic Publishers: Dordrecht, 1996; Vol. 315.

(4) Velev, O. D.; Kaler, E. W. *Adv. Mater.* **2000**, *12*, 531–534.

(5) Velev, O. D.; Jede, T. A.; Lobo, R. F.; Lenhoff, A. M. *Nature* **1997**, *289*, 447–448.

(6) Holland, B. T.; Blanford, C. F.; Stein, A. *Science* **1998**, *281*, 538–540.

(7) Blanco, A.; Chomski, E.; Grabtchak, S.; Ibisate, M.; Hohn, S.; Leonard, S. W.; Lopez, C.; Mesguier, F.; Miguez, H.; Mondia, J. P.; Ozin, G. A.; Toader, O.; van-Driel, H. M. *Nature* **2000**, *405*, 437–440.

(8) Wijnhoven, J. E. G. J.; Zevenhuizen, S. J. M.; Hendriks, M. A.; Vanmaekelbergh, D.; Kelly, J. J.; Vos, W. L. *Adv. Mater.* **2000**, *12*, 888–890.

(9) Braun, P. V.; Wiltzius, P. *Nature* **1999**, *402*, 603–604.

(10) Velv, O. D.; Tessier, P. M.; Lenhoff, A. M.; Kaler, E. W. *Nature* **1999**, *401*, 548–548.

(11) Subramania, G.; Constant, K.; Biswas, R.; Sigalas, M. M.; Ho, K.-M. *Appl. Phys. Lett.* **1999**, *74*, 3933–3935.

(12) Subramanian, B.; Manoharan, V. N.; Thorne, J. D.; Pine, D. J. *Adv. Mater.* **1999**, *11*, 1261–1265.

(13) Trau, M.; A., S. D.; A., A. I. *Science* **1996**, *272*, 706–9.

(14) Holgado, M.; Garcia-Santamaria, F.; Blanco, A.; Ibisate, M.; Cintas, A.; Miguez, H.; Serna, C. J.; Molpeceres, C.; Requena, J.; Mifsud, A.; Mesguier, F.; Lopez, C. *Langmuir* **1999**, *15*, 4701–4704.

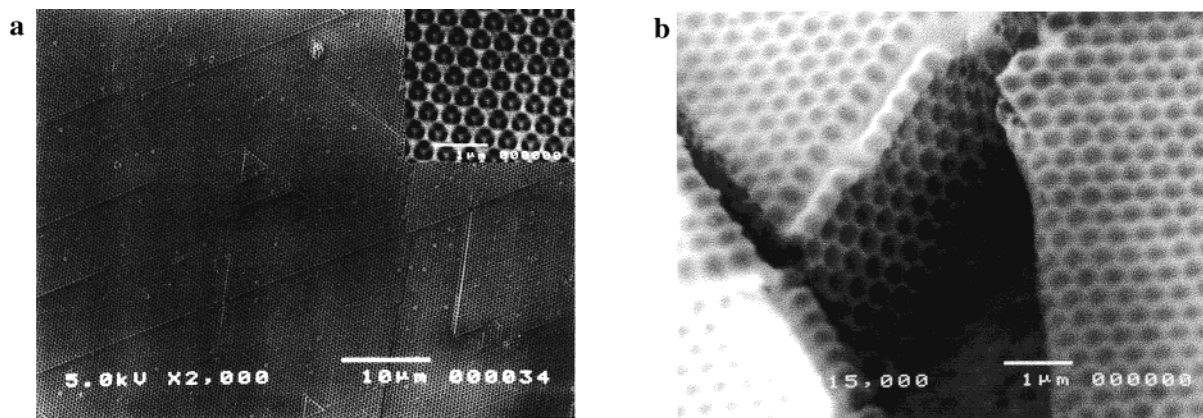


**Figure 1.** SEM images of a silica inverse opal prepared from a 426-nm template: (a) top-view image, (b) cross-sectional image.

of air spheres, can be seen to have the same ordering structure as that of the top layer. Also, the air spheres between neighboring layers are interpenetrated. More information on the bulk structure can be derived from the cross-sectional image (Figure 1b). The ordered arrangement extends from the top surface to the substructure. These results demonstrate that the nanoparticles penetrate throughout the bulk of the opal template without destroying its crystal structure. The three-dimensional CCP crystal structure of the opal template is uniformly replicated. High-quality inverse opal films were also obtained with titania.

All of the samples exhibit flat surfaces, and uniform brilliant colors can be observed if the diffraction of the samples falls in the visible region. To evaluate the possible effect of light absorption and scattering by the nanoparticles themselves, a compact silica film, that is, without voids, was fabricated. This film was colorless and transparent; thus, the absorption and scattering due to the nanoparticles can be neglected. Optical transmittance spectra of the silica inverse opals are shown in Figure 2a, as recorded on a Shimadzu spectrophotometer (UV-3100PC). The spot size of the detecting light was 10 mm × 5 mm. Strong attenuation peaks were observed for all of the samples. The relative stop bandwidth of  $\Delta\lambda/\lambda_0$ , where  $\Delta\lambda$  is the width at half-maximum of the peaks and the  $\lambda_0$  is the center wavelength of the peaks, lies between 6 and 8%, which agrees with the theoretical result, 7.8%, calculated by use of the plane wave method. These results indicate that the highly ordered structure of the inverse opals extends to the millimeter order. The peak positions can be estimated from a simple Bragg diffraction relationship:<sup>16</sup>

$$\lambda = 1.63d(n_a^2 - \sin^2 \theta)^{1/2} \quad (1)$$

where  $\lambda$  is the peak position,  $d$  represents the center-to-center distance between neighboring air spheres, and  $\theta$  the incident angle of the light. The average refractive index,  $n_a$ , is expressed as:  $n_a^2 = n_{\text{silica}}^2(1 - f) + n_{\text{air}}^2f$ , where  $f$  is the volume fraction of air spheres. Four different inverse opal films, with center-to-center distances from 256 to 621 nm were examined. The  $\lambda$  values shift linearly from the visible region to the near-infrared region (Figure 2b). The solid line in Figure 2b was calculated from eq 1, in which the refractive indices of air and silicon dioxide are 1 and 1.5 respectively, and the volume fraction of air spheres was taken to be 0.73, which is the theoretical value expected from the CCP structure. Clearly, the experimental results agree very well with theory. This result strongly supports the conclusion derived from the SEM images that the nanoparticles fill the voids of the opal template completely and that the CCP crystal structure is well replicated.

In conclusion, we have developed an electrophoresis method for the preparation of large, relatively thick inverse opal films

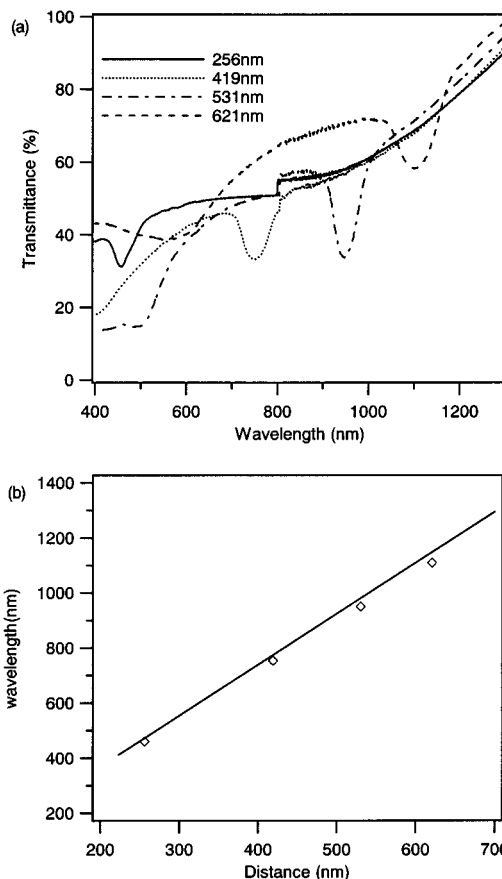


**Figure 2.** (a) Optical transmission spectra of silica inverse opals prepared from templates of various sphere sizes. The light spot was 10 mm × 5 mm. (b) Experimental transmission minima ( $\diamond$ ) as a function of the center-to-center distance, based on the spectra in part (a), together with the theoretically calculated curve (solid line).

with superior optical quality, such that optical transmission spectra were obtained for the first time. Because the external forces on the opal templates were relatively small, their crystal structures were well replicated. The average distance between cracks in the inverse opals was  $\sim 30 \mu\text{m}$ . Although only silica and titania were used in the present work, the electrophoresis technique should be effective for all materials (for example, metals, semiconductors, polymers) from which nanoparticles can be prepared.

**Supporting Information Available:** Synthetic scheme, four SEM images of the silica and titania inverse opals, and mm-scale photographs of samples (PDF). This material is available free of charge via the Internet at <http://pubs.acs.org>.